PAPER

Check for updates

Solvent-tuned magnetic exchange interactions in Dy₂ systems ligated by a μ-phenolato heptadentate Schiff base†

Zhijie Jiang,[ad] Lin Sun,[ac] Min Li,[a] Haipeng Wu,[a] Zhengqiang Xia, [iD] *[a] Hongshan Ke,[a] Yiquan Zhang, [iD] *[b] Gang Xie[a] and Sanping Chen [iD] *[a]

A series of binuclear dysprosium compounds, namely, [Dy(api)]₂ (**1**), [Dy(api)]₂·2CH₂Cl₂ (**2**), [Dy(Clapi)]₂·2C₄H₈O (**3**), and [Dy(Clapi)]₂·2C₃H₆O (**4**) (H₃api = 2-(2-hydroxyphenyl)-1,3-bis[4-(2-hydroxyphenyl)-3-azabut-3-enyl]-1,3-imidazoline; H₃Clapi = 2-(2′-hydroxy-5′-chlorophenyl)-1,3-bis[3′-aza-4′-(2″-hydroxy-5″-chlorophenyl)prop-4′-en-1′-yl]-1,3-imidazolidine), have been isolated by the reactions of salen-type ligands H₃api/H₃Clapi with DyCl₃·6H₂O in different solvent systems. Structural analysis reveals that each salen-type ligand provides a heptadentate coordination pocket (N₄O₃) to encapsulate a Dyᴵᴵᴵ ion and all of the Dyᴵᴵᴵ centers in **1–4** adopt a distorted square antiprism geometry with D_{4d} symmetry. Magnetic studies showed that compound **1** did not exhibit single-molecule magnetic (SMMs) behavior. With the introduction of different lattice solvents, compounds **2–4** showed filed-induced slow magnetic relaxation with barriers U_{eff} of 18.2 K (**2**), 28.0 K (**3**) and 16.4 K (**4**), respectively. *Ab initio* calculations were employed to interpret the magnetization behavior of **1–4**. The combination of experimental and theoretical data reveal the importance of the weak exchange interaction between the Dyᴵᴵᴵ ions in the observation of slow magnetic relaxation, and a relaxation mechanism has been developed to rationalize the observed difference in the U_{eff} values. The different lattice solvents influence Dy–O–Dy bond angles and thus alter the torsion of the square antiprism geometry, consequently resulting in distinct magnetic interactions and the magnetic behavior.

Introduction

Thanks the tremendous optical[1] and magnetic properties of lanthanide ions,[2] the design and study of original lanthanide-based coordination compounds have drawn wide attention in materials chemistry. The slow relaxation of the magnetization in lanthanide-based single-molecule magnets (SMMs) makes them promising and fascinating candidates for molecular magnetism researchers due to their strong spin-orbital coupling

effect and large magnetic anisotropy for constructing SMMs with a higher relaxation energy barrier and blocking temperature.[3–5] Such unique magnetic properties connecting the conventional and quantum world make SMMs good candidates for high-density information storage, quantum information processing and molecular spintronics.[6] Recent rapid advances in this field have led to the design of lanthanide compounds exhibiting very high anisotropic barriers that can reach several thousand wavenumbers,[7–11] as well as magnetic hysteresis up to 80 K,[10,12] making such compounds potential applicants for integration into magnetic memory devices.

Certainly, these forefront advances are concentrated on a single spin center. There are still little investigated on another important factors of molecular magnetism, namely, magnetic exchange interactions and magneto-structural correlations.[13–18] There are mainly the following reasons for the lack of research in this area: the first reason is the deep-seated nature of the 4f orbitals and the associated very weak exchange interactions. The second reason is that it is difficult to understand even the nature of exchange interactions, because the profile of the product of susceptibility and temperature *versus* temperature is dominated by the variation in the population of the Stark levels. The last reason is that ligand changes have no significant effect on the expected magnetic exchange interaction of closely

[a]Key Laboratory of Synthetic and Natural Functional Molecule Chemistry of Ministry of Education, College of Chemistry and Materials Science, Northwest University, Xi'an, Shaanxi 710069, China. E-mail: northwindy@126.com; sanpingchen@126.com

[b]Jiangsu Key Laboratory for NSLSCS, School of Physical Science and Technology, Nanjing Normal University, Nanjing 210023, China. E-mail: zhangyiquan@njnu.edu.cn

[c]College of Chemistry and Chemical Engineering, Henan University, Kaifeng 475001, China

[d]School of Chemistry & Chemical Engineering, Shaanxi Xueqian Normal University, Xi'an 710100, China

analogues. For the above reasons, little research has been done on the understanding of exchange interactions in closely related lanthanide compounds.

Compared to mononuclear lanthanide compounds known as single-ion magnets (SIMs), dilanthanide species are viewed as the simplest molecular units to conveniently study the nature and strength of magnetic exchange interactions between spin carriers and then elucidate magnetic relaxation mechanisms.[19-21] In recent years, different kinds of ligands including phthalocyanine,[22] Schiff base,[23] β-diketone,[24] carboxylic acid[25] and their derivatives have been successfully utilized to construct binuclear lanthanide compounds. Among them, Schiff base ligands with versatile O, N-based multi-chelating sites to impart different ligand fields and bridges have invoked increasing interest in the study of the magnetic anisotropy and exchange interactions of binuclear systems. Based on above all, two heptadentate Schiff base ligands has been elected to prepared four closely related Dy_2 compounds, with the formula $[Dy(Xapi)]_2 \cdot 2Y$, (X = H (**1**, **2**), Cl (**3**, **4**); Y = no solvent (**1**), CH_2Cl_2 (**2**), C_4H_8O (**3**), C_3H_6O (**4**); H_3api = 2-(2-hydroxyphenyl)-1,3-bis[4-(2-hydroxyphenyl)-3-azabut-3-enyl]-1,3-imidazoline; H_3Clapi = 2-(2′-hydroxy-5′-chlorophenyl)-1,3-bis[3′-aza-4′-(2″-hydroxy-5″-chlorophenyl)prop-4′-en-1′-yl]-1,3-imidazolidine). Magnetic properties measurements indicate that the slight changes of coordination geometry around the Dy^{III} induced by the guest solvent molecules produce different coupling interactions and distinct magnetic behaviour. *Ab initio* calculations are employed to interpret the magnetic anisotropy and exchange interactions of the compounds and the results give a more thorough understanding of the effects of structural factors on the relaxation dynamics in Dy_2^{III} SMMs.

Experimental

Materials and methods

All commercial reagents and solvents were purchased from Aldrich, Adamas and TCI and were used without further purification. ^{1}H-NMR spectra were recorded on a Bruker AV-400 or AV-100 spectrometer. Chemical shifts (δ) reported in parts per million (ppm) are referenced relative to the residual solvent peak in the NMR solvent ($CDCl_3$: δ 7.26 ($CHCl_3$)). Data are represented as follows: chemical shift, multiplicity (s = singlet, d = doublet, t = triplet, q = quartet, m = multiplet), integration, and coupling constants in Hertz (Hz). The phase purity of the bulk samples was confirmed by powder X-ray diffraction (PXRD) measurements executed on a Rigaku RU200 diffractometer at 60 kV, 300 mA, and Cu Kα radiation (l = 1.5406 Å), with a scan speed of 51 min^{-1} and a step size of 0.02° in 2θ. Magnetic measurements were performed in the temperature range of 2.0–300 K under 0 Oe, using a Quantum Design MPMS-XL-7 SQUID magnetometer on polycrystalline samples. The diamagnetic corrections for the complexes were estimated using Pascal's constants. Alternating current (ac) susceptibility experiments were performed using an oscillating ac field of 0 Oe at ac frequencies ranging from 1.0 to 1000 Hz. The magnetization was measured in the field range of 0–70 000 Oe.

Synthetic procedures

Schiff base ligand H_3api. To a stirred solution of salicylaldehyde (1.83 g, 15 mmol) in methanol (20 ml) at 0 °C, trien (0.73 g, 5 mmol) was dropwise added at 0–5 °C. Then the mixture was heated at 65 °C for three hours. After being cooled to room temperature, yellow solid was separated by filtration and washed with diethyl ether to afford H_3api (1.7 g, 75%) (Scheme 1).

^{1}H NMR (400 MHz, $CDCl_3$) δ 13.21 (br s, 2H, OH_{18}), 10.66 (br s, 1H, OH_{19}), 8.25 (s, 2H, H_5), 7.31–7.29 (m, 2H, H_9), 7.25 (d, J = 6.9 Hz, 2H, H_7), 7.22 (m, 2H, H_{13} & H_{15}), 7.01 (m, 1H, H_{14}), 6.93 (d, J = 8.3 Hz, 2H, H_{10}), 6.86 (t, J = 7.4 Hz, 2H, H_8), 6.82–6.79 (m, 1H, H_{16}), 3.84 (s, 1H, H_4), 3.60 (t, J = 6.5 Hz, 4H, H_3), 3.43 (q, J = 4.7 Hz, 2H, $H_1^{eq.}$), 2.97 (dt, J = 12.7, 6.4 Hz, 2H, $H_2^{eq.}$), 2.73–2.63 (m, 4H, H_1^{ax} & H_2^{ax})(Fig. S1†).

^{13}C {^{1}H} NMR (101 MHz, $CDCl_3$) δ 166.2 (C_5), 161.2 (C_{11}), 158.4 (C_{17}), 132.4 (C_9), 131.5 (C_7), 131.0 (C_{13}), 130.4 (C_{15}), 121.0 (C_6), 118.86 (C_{14}), 118.85 (C_{12}), 118.7 (C_8), 117.13 (C_{10}), 117.09 (C_{16}), 89.8 (C_4), 58.6 (C_3), 53.0 (C_2), 51.3 (C_1) (Fig. S2†).

Schiff base ligand H_3Clapi. To a stirred solution of 5-chlorosalicylaldehyde (2.35 g, 15 mmol) in methanol (30 ml) at 0 °C, trien (0.73 g, 5 mmol) was added dropwise at 0–5 °C. Then, the mixture was heated at 65 °C for six hours. After being cooled to room temperature, the yellow solid was separated by filtration and washed with diethylether to afford H_3Clapi (2.2 g, 79%).

^{1}H NMR (400 MHz, $CDCl_3$) δ 13.07 (br s, 2H, OH_{18}), 10.43 (br s, 1H, OH_{19}), 8.17 (s, 2H, H_5), 7.23 (dd, J = 8.8, 2.4 Hz, 2H, H_9), 7.18 (d, J = 2.4 Hz, 2H, H_7), 7.15 (d, J = 2.4 Hz, 1H, H_{15}), 6.96 (d, J = 2.4 Hz, 1H, H_{13}), 6.87 (d, J = 8.8 Hz, 2H, H_{10}), 6.68 (d, J = 8.7 Hz, 1H, H_{16}), 3.79 (s, 1H, H_4), 3.59 (t, J = 6.1 Hz, 4H, H_3), 3.44–3.40 (m, 2H, $H_1^{eq.}$), 2.99–2.92 (m, 2H, $H_2^{eq.}$), 2.73–2.64 (m, 4H, H_1^{ax} & H_2^{ax}) (Fig. S3†).

^{13}C {1H} NMR (101 MHz, $CDCl_3$) δ 165.2 (C_5), 159.8 (C_{11}), 156.9 (C_{17}), 132.3 (C_9), 130.7 (C_7), 130.34 (C_{13}), 130.28 (C_{15}), 123.4 (C_{14}), 123.3 (C_8), 122.5 (C_6), 119.6 (C_{12}), 118.7 (C_{10}), 118.6 (C_{16}), 89.0 (C_4), 58.3 (C_3), 52.8 (C_2), 51.2 (C_1) (Fig. S4†).

[Dy(api)]$_2$ (1). A mixture of H_3api (0.05 mmol, 22.93 mg) and Et_3N (0.1 mmol, 0.014 ml) in methanol (15 ml) was kept stirring for two hours, to which $DyCl_3 \cdot 6H_2O$ (0.05 mmol, 18.85 mg) was added. The mixed solution above was stirred for three hours. After filtration, the resultant solution was kept at room

Scheme 1 Probable mechanism for the formation of the ligand H_3api.

temperature (Scheme 2). Pale-yellow blocky crystals were gathered after one week in a yield of 32% (based on Dy^{III} salts). Elem. anal. calcd: C, 52.47; H, 4.40; N, 9.07%. Found: C 52.33; H 4.41; N 9.05%.

[Dy(api)]$_2$·2CH$_2$Cl$_2$ (2). Compound **2** was obtained from the following two ways (Scheme 2):

(i) The synthesis method of compound **2** is similar to that of compound **1**, except that it is replaced with the mixed methanol (5 ml) and dichloromethane (10 ml). Pale-yellow blocky crystals were gathered after three days in a yield of 28% (based on Dy^{III} salts). Elem. anal. calcd: C, 47.84; H, 4.16; N, 7.97%. Found: C 47.79; H 4.15; N 7.95%.
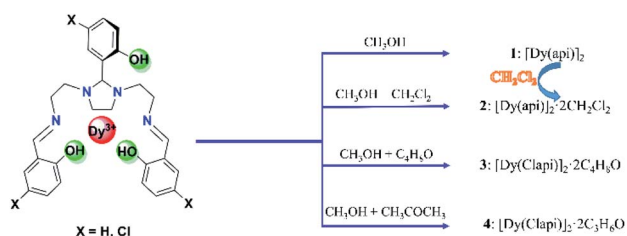
(ii) Single crystals of compound **1** (1.0 mmol, 0.277 g) were soaked into dichloromethane solution (30 ml), which also yielded pale-yellow blocky crystals of compound **2** within one week at room temperature (Scheme 2).

[Dy(Clapi)]$_2$·2C$_4$H$_8$O (3). A mixture of H$_3$Clapi (0.05 mmol, 28.10 mg) and Et$_3$N (0.1 mmol, 0.014 ml) in methanol (5 ml) and tetrahydrofuran (10 ml) was kept stirring for two hours, to which DyCl$_3$·6H$_2$O (0.05 mmol, 18.85 mg) was added. The mixed solution above was stirred for three hours. After filtration, the resultant solution was kept at room temperature (Scheme 2). Pale-yellow blocky crystals were gathered after four days in a yield of 54% (based on Dy^{III} salts). Elem. anal. calcd: C, 46.93; H, 4.07; N, 7.06%. Found: C 46.91; H 4.07; N 7.04%.

[Dy(Clapi)]$_2$·2C$_3$H$_6$O (4). The synthesis method of compound **4** is similar to that of compound **3**, except that it is replaced with the mixed methanol (5 ml) and acetone (10 ml) (Scheme 2). Pale-yellow blocky crystals were gathered after two days in a yield of 51% (based on Dy^{III} salts). Elem. anal. calcd: C, 46.23; H, 3.88; N, 7.19%. Found: C 46.21; H 3.87; N 7.21%.

X-ray crystallography

The crystal data for all compounds in our system have been collected on a Bruker SMART APEX-CCD-based diffractometer (Mo Kα radiation, $\lambda = 0.710\,73$ Å) at low temperature. Raw area detector data integration and reduction were performed with SAINT$^+$ program. Absorption correction based on multiscan was processed using the SADABS software.[26] All structures were solved by the direct methods and refined by a full-matrix least-squares method on F^2 using the SHELXL-2014 software.[27] Non-hydrogen atoms were refined with anisotropic thermal parameters. The experimental details of crystal data, data collection parameters, and refinement statistics are presented in Table S1,† and the selected bond lengths and angles are summarized in Table S2.†

Scheme 2 Syntheses of Dy$_2$ compounds **1–4**.

Computational methodology

Theoretical studies using CASSCF calculations on the Dy^{III} nodes in four compounds based on the single-crystal diffraction measured geometries were performed by MOLCAS 8.0 software package.[28,29] For the calculations, the basis sets are atomic natural orbitals from the MOLCAS ANO-RCC library: ANO-RCCVTZP for Dy^{III} cation; VTZ for close N atom and O atom; VDZ for distant atoms. The calculations used the second-order Douglas–Kroll–Hess Hamiltonian, in which scalar relativistic contractions were adopted in the basis sets. The spin–orbit coupling was treated individually in the RASSI process. In the CASSCF calculations, the active electrons in seven active spaces contain all f electrons CAS (9 in 7) for all compounds. All the roots were computed in the active space to eliminate possible doubts. The maximal value of spin-free state has been mixed, which might be related with the computer hardware (all from 21 sextets, 128 from 224 quadruplets and 130 from 490 doublets for Dy^{III} nodes).

Results and discussion

Synthesis and characterization of ligand H$_3$api

The ligand H$_3$api is prepared from the condensation of triethylenetetramine and salicylaldehyde in 1 : 3 molar ratio in methanol and characterized by ^{1}H and ^{13}C NMR spectroscopic techniques. It is noted that in these Schiff bases ligand, five-membered imidazolidine rings were formed at the backbone after the condensation and that the middle arm was, therefore, unique from the other two arms (clearly shown in the ^{1}H NMR spectra). Two phenol hydroxyl resonances were observed at about 10 and 13 ppm in a 1 : 2 ratio. These two downfield signals can be explained by the intramolecular hydrogen bonding of the phenol hydroxyl with unsaturated azomethine nitrogen or tertiary nitrogen which caused decrease in the shielding at the hydroxy hydrogen. However, OH resonances on the terminal outside arms are further downfield than that of the middle arm. The explanation is that, for the terminal arm, the O–H···N group lies coplanar with the aromatic ring; hence, the proton is further deshielded by the induced aromatic ring current.

A plausible mechanism was proposed for generating ligand H$_3$api (Scheme 1). First, the reaction between triethylenetetramine and salicylaldehyde, thus producing the precursor A. The nucleophilic addition of A to another salicylaldehyde gives the intermediate B, which can be converted into the imidazolidine ring compound H$_3$api through the internal S_N^2 reaction.

Preparation and structural description of 1–4

Incorporating the ligand H$_3$api/H$_3$Clapi with DyCl$_3$·6H$_2$O in different solvents containing an excess of triethylamine brings about four binuclear Dy^{III} species share the formula [DyXapi]$_2$·solvent (Scheme 2): [Dyapi]$_2$ (**1**), [Dy(api)]$_2$·2CH$_2$Cl$_2$ (**2**), [Dy(Clapi)]$_2$·2C$_4$H$_8$O (**3**) and [Dy(Clapi)]$_2$·2C$_3$H$_6$O (**4**), respectively. Because each ligand carries a triple negative charge, the positive charge of the two trivalent Dy^{III} is counterbalanced and the binuclear compounds are neutral; hence no counterions are

necessary and these symmetric Dy_2 compounds are structurally similar. Instead of forcing N_4O_3 donor atoms exclusively from one ligand onto one metal ion, here the homodinuclear compounds contain two Dy^{III} ions where each of the metal ions is coordinated by two N_2O donor sets, each coming from one ligand. Two phenolate oxygen atoms, from the middle arm of each ligand, act as μ-bridges between the two metal centres and complete the eight-membered coordination sphere, overall furnishing a sandwich type dimeric structure. This no doubt arises from the rigid five-membered imidazolidine ring in the ligand backbone; this forces the ligand into a more open configuration rendering impossible coordination of all the donor atoms of one ligand to one metal ion. Instead, these two ligands cooperate with each other to form two compartments to accommodate two Dy^{III} (Fig. 1a).

The distortions from the ideal eight-coordinate geometries for the $\{DyN_4O_4\}$ core is computed using SHAPE 2.1 software[30] and the least deviation has been found for the distorted square antiprism geometry, suggesting the presence of pseudo-D_{4d} symmetry (Fig. 1b) for the core geometry but with different distortions from the ideal geometry (Table S3†). The Dy–N (imidazolidine) bond lengths are approximately 0.3 Å larger than the Dy–N (imine) bond lengths in all the cases (Table S2†).

The unit cell of compound **2** contains binuclear units with two dichloromethane molecules in the crystal lattice for each dimer, and each compound **3** and **4** has two solvent molecules tetrahydrofuran and acetone. But no free solvent molecules in compound **1**. Because of the uncoordinated solvent molecules and, most importantly, the different coordination geometry, the supramolecular interactions are different in the structures. The

3D Hirshfeld surface analysis and 2D fingerprint plot of **1–4** were applied to analyze the intermolecular interactions. As illustrated in Fig. S7–S10,† the major contribution (73.6% for **1**, 58.5% for **2**, 50.1% for **3** and 41.7% for **4**) is provided by weak van der Waals H···H interactions, while C–H···Cl hydrogen-bond interactions provide partial contributions of 18.5%, 24.2% and 28.8% for **2–4**, respectively.

Magnetic studies

For all samples, the variable-temperature dc susceptibility measurements were performed at an applied field of 1000 Oe from 2 to 300 K (Fig. 2); the variable-field magnetization measurements were performed at 2 K, 3 K and 5 K from 0 to 7 T (Fig. S11†). In summary, the general behaviour of all compounds is consistent with other Dy^{III} compounds reported in the literature.[31–33]

Direct-current (dc) magnetic susceptibilities

The room temperature $\chi_M T$ value for all compounds (see Fig. 2) is in good agreement with the expected value for two noninteracting Dy^{III} ions ($^7H_{15/2}$, $S = 5/2$, $L = 5$, $g = 4/3$, $C = 14.17$ cm^3 K mol^{-1}).[34] As the temperature decreases, $\chi_M T$ is almost constant down to ~50 K and then slightly decreases to reach a minimum at 2 K, which could be ascribed to an intramolecular antiferromagnetic exchange coupling between the two Dy^{III} ions. The $M = f(\mu_0 H)$ curve increases with the applied magnetic field and reaches saturation at 7 T. It is possible to fit the susceptibility and the magnetization data (see Fig. S11†) using a model based on the spin Hamiltonian $H = -JS_{Dy_1} \times S_{Dy_2} + g\beta H_z S_z$, where g is the Lande factor and J the interaction parameter between the local $S = 15/2$ spins of the Dy^{III} ions.

Ac susceptibility measurements

In order to probe the magnetic dynamic behaviour of these compounds, the ac susceptibilities at various frequencies and temperatures measurements were performed. Under zero
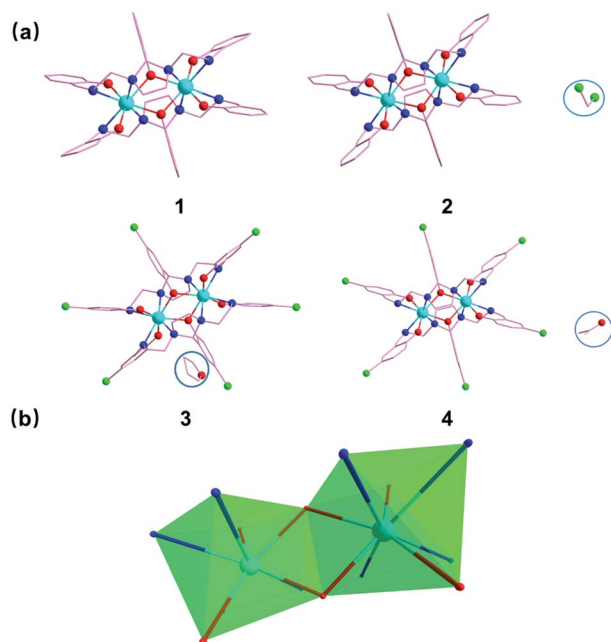

Fig. 1 (a) X-ray crystal structure of compounds of **1–4**. (b) Local coordination polyhedron of the Dy^{III} ions in **1–4**. Color code: cyan = Dy^{III}; green = Cl; red = O; blue = N. Hydrogen atoms and carbon atom are omitted for clarity.
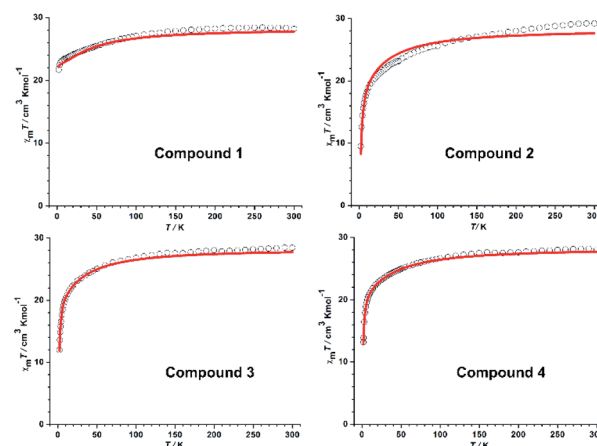

Fig. 2 $\chi_M T$ vs. T plots for **1–4** (red solid lines represent the simulation from *ab initio* calculation).

applied dc field, both the in-phase (χ') and out-of-phase (χ'') susceptibilities did not display a frequency and temperature dependence for all samples in our system. Lanthanide ions are well known to exhibit significant quantum tunnelling of the magnetization (QTM), but in the case of Dy^{III} ions, the QTM is reduced as a result of a spin-parity effect. The spin-parity effect predicts that the QTM should be suppressed at zero field when the total spin of the magnetic system is a half-integer but allowed in integer-spin systems. However, QTM can be induced experimentally even in half-integer spin systems through effects such as environmental degrees of freedom as well as hyperfine and dipolar coupling *via* transverse field components.[35] In order to suppress or minimize the QTM, optimum dc field measurements were carried out at optimum fields of 1500 Oe for **2**, 700 Oe for **3** and 500 Oe for **4**, respectively (Fig. 3). Subsequent ac measurements were carried out at these optimum fields, both χ' and χ'' susceptibilities show significant frequency dependence peaks at a relatively high temperature range, which clearly indicates that the SMMs behaviour of compounds **2**, **3** and **4** (Fig. S12–S14†). In contrast, compound **1** display no out-of-phase component of the ac susceptibilities in the applied field for frequencies of 1 and 1000 Hz down to 2 K (Fig. S12 and S13†). Really, in such measurements the degeneracy of the $\pm M_S$ energy levels can be removed, consequently preventing the tunnelling of electrons from the $+M_S$ state to the $-M_S$ state through the spin-reversal barrier. The frequency magnitude of the first maximum peaks for all compounds reflect the impact of QTM on the SMMs, where the lower one mostly indicates the existence of a slower QTM process where the thermally activated Orbach relaxation process occurs prominently.

The Cole–Cole plots[36] for all samples are shown in Fig. 4 and exhibit semicircular shape which can be fitted to the generalized Debye model. The fitting parameters τ (relaxation time) and α (α determines the width of the distribution of relaxation times) are given in Table S4.† The α values are <0.25 in the higher temperature regions for **2** and **4**, indicating the presence of a relatively narrow width of relaxation processes most likely due to a combination of QTM and thermally assisted relaxation pathways. The presence of multiple relaxation processes is possible, as reported in other literatures.[37–39] For compound **3**, the α values are <0.05 which indicates a single relaxation mechanism. The thermally induced relaxation can be fit using the Arrhenius law ($\tau = \tau_0 \exp(U_{eff}/kT)$) yielding effective energy barriers and extrapolated relaxation times were $U_{eff} = 18.19$ K, $\tau_0 = 10.9 \times 10^{-6}$ (**2**) under 1500 dc field, 27.99 K, $\tau_0 = 2.92 \times 10^{-6}$ (**3**) under 700 dc field and 16.35 K, $\tau_0 = 12.6 \times 10^{-6}$ (**4**) under 500 dc field (Fig. 4). These relaxation barriers are comparable to those of other reported similar Dy_2 SMMs,[40] suggesting that the slow relaxation behavior of **2–4** originates primarily from the presence of anisotropic Dy^{III} ions. The magnetic coupling between lanthanide ions as a secondary consideration may also mediate the magnetic relaxation of Dy_2 compounds.

Structure–property relationship

Although compounds **1–4** show a very similar crystal structure, they exhibit different magnetic relaxation behaviours. To probe the structure–property relationship in all samples, some crucial parameters of structure and property, including Dy–O–Dy angles in Dy_2O_2 core, the CShM of D_{4d}, and U_{eff} have been presented in Fig. S15.† These distinctive magnetic behaviours must be caused by subtle but crucial differences among the respective structures. According to the single crystal X-ray diffraction study and the semiquantitative method of polytopal analysis, for compounds **1–4**, the most reasonable geometry around the Dy atom is D_{4d}. However, on a closer comparison of the four Dy_2 structures, the Dy–O–Dy angles are found to be slightly different. The Dy–O–Dy angle of compound **3** is 110.509°, which is a bit smaller than other three (**1**, 111.027; **2**, 110.596; **4**, 110.626, respectively). Whereas **1** shows the largest Dy–O–Dy angle. These slight differences of important bond angles may have an influence on the distorted degree of the coordination geometry of the Dy^{III} ion, which can lead to the fast quantum tunnelling arising introduced by a geometrical distortion of the coordinated sphere. These differences can also have a significant influence on the magnetic interaction between the Dy^{III} ions. Additionally, considering that the single-ion anisotropy contributions from the two Dy^{III} centers in the bimetallic units are symmetry related, the CSM method was employed to evaluate the deviation from an ideal square antiprism geometry geometry. Herein, the larger the calculated CSAPR-8 parameter, the greater the deviation from an ideal D_{4d} symmetry. The calculated CSAPR-8 parameters are 1.423, 1.318, 1.268 and 1.389 for compounds **1–4**, respectively, indicating the largest deviation from the ideal symmetry for **1**. It is evident that the introduction of guest molecules in **2**, **3** and **4** induces decreased Dy–O–Dy angles and enhanced symmetry, and thus triggering the SMM behaviour for the compounds. The improvement of SMM property of Dy_2 complex by introducing free molecule has been observed in some reported systems.[19b,41] However, there are no clear electronic effects on the magnetic relaxation behaviors between **1–2** and **3–4** induced by the different substituents (–H or –Cl) of terminal ligands.

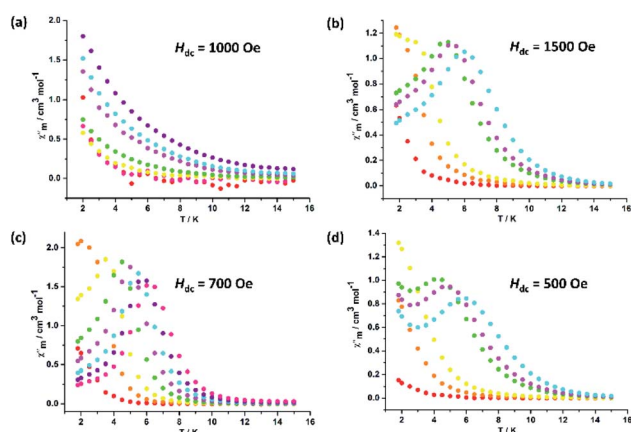Further insights into the electronic structure and magnetic blocking in the present dysprosium complexes were obtained

Fig. 3 Temperature dependence of the out-of-phase ac susceptibility signals under an applied dc field for **1** (a), **2** (b), **3** (c) and **4** (d).
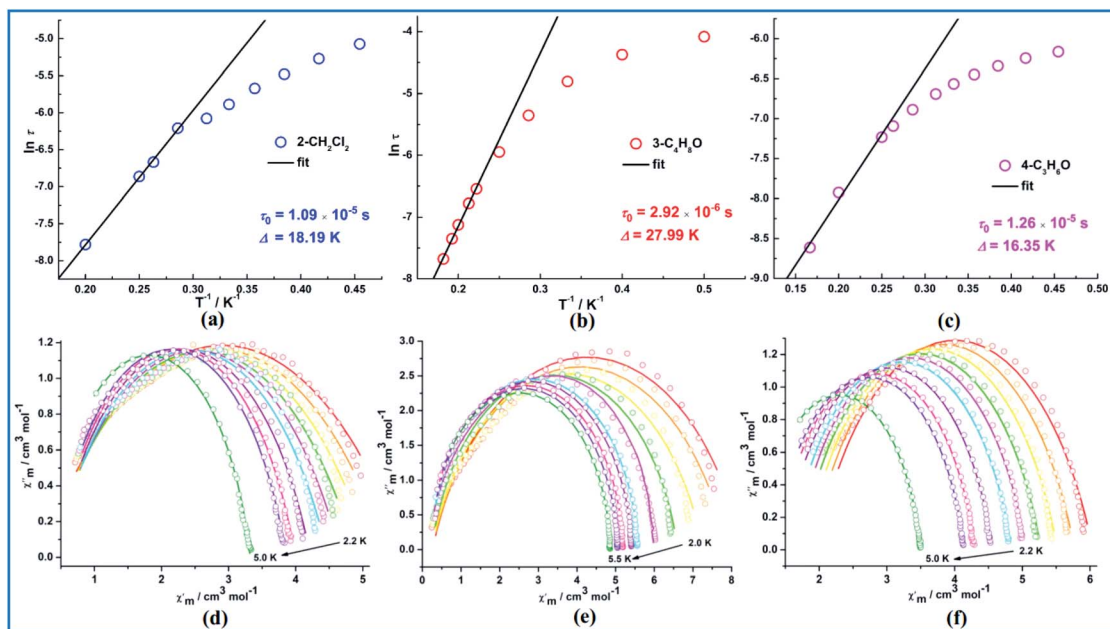
Fig. 4 The Arrhenius plots constructed from the ac magnetization relaxation dynamics under an indicated dc field for **2** (a), **3** (b) and **4** (c). The solid lines represent the fitting with the Arrhenius law. Cole–Cole diagram under 1500 Oe dc field for **2** (d), under 700 Oe dc field for **3** (e) and under 500 Oe dc field for **4** (f). The solid lines represent the best fit to the measured results.

via ab initio calculations. *Ab initio* CASSCF/RASSI/ SINGLE_ANISO calculations have been carried out with MOL-CAS 8.0 (ref. 28 and 29) on individual Dy^{III} fragments of compounds **1–4** on the basis of X-ray determined structures (see the ESI† for details). Each Dy centre was calculated, keeping the experimentally determined structure of the corresponding complex while replacing the neighbouring Dy^{III} ion with diamagnetic Lu. The lowest Kramers doublets and the g tensors corresponding to the pseudospin $S = 1/2$ of Dy^{III} ions for all compounds are shown in Table S5.† Herein, the calculated g_z values of the Dy^{III} fragments of **1–4** are close to 20, which shows that the Dy^{III}–Dy^{III} exchange interactions for each of them can be approximately regarded as the Ising type.

The magnetic susceptibilities of compounds **1–4** were simulated with the program POLY_ANISO[42] using the exchange parameters from Table 1. All parameters were calculated with respect to the pseudospin $S = 1/2$ of the Dy ions. From Table 1, the slight differences of the $J_{dipolar}$ values are found in complexes **1–4**, and the J_{exch} is ferromagnetic for **1** whereas antiferromagnetic for **2–4**, the total interaction J in **2–4** being around 10 times larger than that in **1**. The Dy^{III}–Dy^{III}

interactions J of all compounds within the Lines model[43,44] are antiferromagnetic. The distinct magnetic interactions observed for complexes **1** and **2–4** are most likely induced by different Dy–O–Dy angles. And the total coupling parameters J (dipolar and exchange) were included to fit the magnetic susceptibilities. As shown in Fig. 2, a great agreement was reached between the calculated and experimental $\chi_M T$ versus T plots of **1–4**. The main magnetic axes on the Dy^{III} ions for **1–4** are indicated in Fig. S17,† where the magnetic axes on Dy^{III} for each compound are antiparallel to each other because of the Dy^{III}–Dy^{III} antiferromagnetic interaction.

The foregoing results clearly reveal the origin of the magnetization dynamics: (a) the similar energy barriers are mainly from the single-ion anisotropy of the Dy^{III} centres because of the similar coordination environments; (b) the subtle differences caused by either the guest molecules or no guest molecule lead to different magnetic interactions and symmetry which tune the relaxation rate to give different effective relaxation barriers. The weaker magnetic interactions and lower symmetry of the coordination geometry for **1** most likely associate with the poorer SMMs behavior than **2–4**. This is a typical example in which guest molecules are employed to adjust the molecule symmetry as well as the magnetic interactions between lanthanides and thereby tune the relaxation rates arising from incoherent quantum tunnelling of the magnetization.

Conclusions

A series of Dy₂ SMMs were prepared as well as characterized structurally and magnetically. The structural analyses

Table 1 Fitted exchange coupling constant J_{exch}, the calculated dipole–dipole interaction $J_{dipolar}$, the total J and intermolecular interactions zJ' between Dy^{III} ions in compounds **1–4** (cm^{-1})

Compound	1	2	3	4
$J_{dipolar}$	−2.56	−2.51	−2.47	−2.69
J_{exch}	2.25	−1.25	−0.50	−0.50
J	−0.31	−3.76	−2.97	−3.19

demonstrated that we successfully prevented the coordination of solvent molecules to Dy^{III} ions utilizing the larger steric hindrance of Schiff base ligand api^{3-}, and gave rise to the D_{4d} analogues with enhanced local symmetry and enhanced U_{eff}. The different anisotropy of individual Dy^{III} ions and intra-molecular couplings are most likely derived from the different local symmetry, which ultimately leads to different SMM behaviors. The work verifies the sensitivity of magnetic relaxation to the remote alteration on individual spin centers, which provides an opportunity to shed light on tuning of the magnetic properties of SMMs.

Conflicts of interest

There are no conflicts to declare.

Acknowledgements

Notes and references

1 K. Binnemans, *Coord. Chem. Rev.*, 2009, **109**, 4283–4374.
2 J. Luzon and R. Sessoli, *Dalton Trans.*, 2012, **41**, 13556–13567.
3 (*a*) N. Ishikawa, M. Sugita, T. Ishikawa, S. Koshihara and Y. Kaizu, *J. Am. Chem. Soc.*, 2003, **125**, 8694–8695; (*b*) M. A. AlDamen, J. M. Clemente-Juan, E. Coronado, C. MartiGastaldo and A. Gaita-Arino, *J. Am. Chem. Soc.*, 2008, **130**, 8874–8875; (*c*) S. D. Jiang, B. W. Wang, G. Su, Z. M. Wang and S. Gao, *Angew. Chem., Int. Ed.*, 2010, **49**, 7448–7451; (*d*) D. N. Woodruff, R. E. P. Winpenny and R. A. Layfield, *Chem. Rev.*, 2013, **113**, 5110–5148; (*e*) H. C. Wu, B. Yan, H. F. Li, V. Singh, P. T. Ma, J. Y. Niu and J. P. Wang, *Inorg. Chem.*, 2018, **57**, 7665–7675; (*f*) P. Zhang, Y. N. Guo and J. K. Tang, *Coord. Chem. Rev.*, 2013, **257**, 1728–1763; (*g*) D. D. Yin, Q. Chen, Y. S. Meng, H. L. Sun, Y. Q. Zhang and S. Gao, *Chem. Sci.*, 2015, **6**, 3095–3101; (*h*) W. B. Sun, P. F. Yan, S. D. Jiang, B. W. Wang, Y. Q. Zhang, H. F. Li, P. Chen, Z. M. Wang and S. Gao, *Chem. Sci.*, 2016, **7**, 684–691; (*i*) Y. N. Guo, L. Ungur, G. E. Graroth, A. K. Powell, C. J. Wu, S. E. Nagler, J. K. Tang, L. F. Chibotaru and D. M. Cui, *Sci. Rep.*, 2014, **4**, 5471–5477; (*j*) H. L. Wang, B. W. Wang, Y. Z. Bian, S. Gao and J. Z. Jiang, *Coord. Chem. Rev.*, 2016, **306**, 195–216; (*k*) R. J. Blagg, L. Ungur, F. Tuna, J. Speak, P. Comar, D. Collison, W. Wernsdorfer, E. J. L. McInnes, L. F. Chibotaru and R. E. P. Winpenny, *Nat. Chem.*, 2013, **5**, 673–678; (*l*) D. S. Krylov, F. Liu, S. M. Avdoshenko, L. Spree, B. Weise, A. Waske, A. U. B. Wolter, B. Büchner and A. A. Popov, *Chem. Commun.*, 2017, **53**, 7901–7904; (*m*) X. J. Zhang, S. Liu, V. Vieru, N. Xu, C. Gao, B. W. Wang,

W. Shi, L. F. Chibotaru, S. Gao, P. Cheng and A. K. Powell, *Chem.–Eur. J.*, 2018, **24**, 6079–6086; (*n*) P. Zhang, L. Zhang, C. Wang, S. F. Xue, S. Y. Lin and J. K. Tang, *J. Am. Chem. Soc.*, 2014, **136**, 4484–4487.
4 (*a*) Y. C. Chen, J. L. Liu, L. Ungur, J. Liu, Q. W. Li, L. F. Wang, Z. P. Ni, L. F. Chibotaru, X. M. Chen and M. L. Tong, *J. Am. Chem. Soc.*, 2016, **138**, 2829–2837; (*b*) P. T. Ma, F. Hu, Y. Huo, D. D. Zhang, C. Zhang, J. Y. Niu and J. P. Wang, *Cryst. Growth Des.*, 2017, **17**, 1947–1956; (*c*) P. T. Ma, F. Hu, R. Wan, Y. Huo, D. D. Zhang, J. Y. Niu and J. P. Wang, *J. Mater. Chem. C*, 2016, **4**, 5424–5433; (*d*) P. T. Ma, R. Wan, Y. N. Si, F. Hu, Y. Y. Wang, J. Y. Niu and J. P. Wang, *Dalton Trans.*, 2015, **44**, 11514–11523; (*e*) P. E. Kazin, M. A. Zykin, V. V. Utochnikova, O. V. Magdysyuk, A. V. Vasiliev, Y. V. Zubavichus, W. Schnelle, C. Felser and M. Jansen, *Angew. Chem., Int. Ed.*, 2017, **56**, 13416–13420; (*f*) S. Demir, M. D. Boshart, J. F. Corbey, D. H. Woen, M. I. Gonzalez, J. W. Ziller, K. R. Meihaus, J. R. Long and W. J. Evans, *Inorg. Chem.*, 2017, **56**, 15049–15056.
5 (*a*) L. Norel, L. E. Darago, B. L. Guennic, K. Chakarawet, M. I. Gonzalez, J. H. Olshansky, S. Rigaut and J. R. Long, *Angew. Chem., Int. Ed.*, 2018, **57**, 1933–1938; (*b*) Y. S. Meng, L. Xu, J. Xiong, Q. Yuan, T. Liu, B. W. Wang and S. Gao, *Angew. Chem., Int. Ed.*, 2018, **57**, 4673–4676; (*c*) K. Wang, F. Ma, D. D. Qi, X. Chen, Y. X. Chen, Y. C. Chen, H. L. Sun, M. L. Tong and J. Z. Jiang, *Inorg. Chem. Front.*, 2018, **5**, 939–943; (*d*) Z. J. Jiang, L. Sun, Q. Yang, B. Yin, H. S. Ke, J. Han, Q. Wei, G. Xie and S. P. Chen, *J. Mater. Chem. C*, 2018, **6**, 4273–4280; (*e*) K. Katoh, S. Yamashita, N. Yasuda, Y. Kitagawa, B. K. Breedlove, Y. Nakazawa and M. Yamashita, *Angew. Chem., Int. Ed.*, 2018, **130**, 9406–9411.
6 (*a*) R. Sessoli, D. Gatteschi, A. Caneschi and M. A. Novak, *Nature*, 1993, **365**, 141–143; (*b*) R. Sessoli and A. K. Powell, *Coord. Chem. Rev.*, 2009, **253**, 2328–2341; (*c*) H. L. C. Feltham and S. Brooker, *Coord. Chem. Rev.*, 2014, **276**, 1–33; (*d*) S. Demir, I. R. Jeon, J. R. Long and T. D. Harris, *Coord. Chem. Rev.*, 2015, **289–290**, 149–176; (*e*) L. Ungur, S.-Y. Lin, J. Tang and L. F. Chibotaru, *Chem. Soc. Rev.*, 2014, **43**, 6894–6905; (*f*) Y.-S. Meng, S.-D. Jiang, B.-W. Wang and S. Gao, *Acc. Chem. Res.*, 2016, **49**, 2381–2389; (*g*) J.-H. Jia, Q.-W. Li, Y.-C. Chen, J.-L. Liu and M.-L. Tong, *Coord. Chem. Rev.*, 2017, **378**, 365–381; (*h*) M. Feng and M.-L. Tong, *Chem.–Eur. J.*, 2018, **24**, 7574–7594; (*i*) J.-L. Liu, Y.-C. Chen and M.-L. Tong, *Chem. Soc. Rev.*, 2018, **47**, 2431–2453; (*j*) W.-P. Chen, P.-Q. Liao, Y. Yu, Z. Zheng, X.-M. Chen and Y.-Z. Zheng, *Angew. Chem., Int. Ed.*, 2016, **55**, 9375–9379.
7 J. Liu, Y.-C. Chen, J.-L. Liu, V. Vieru, L. Ungur, J.-H. Jia, L. F. Chibotaru, Y. Lan, W. Wernsdorfer, S. Gao, X.-M. Chen and M.-L. Tong, *J. Am. Chem. Soc.*, 2016, **138**, 5441–5450.
8 S. K. Gupta, T. Rajeshkumar, G. Rajaraman and R. Murugavel, *Chem. Sci.*, 2016, **7**, 5181–5191.
9 L. Ungur and L. F. Chibotaru, *Inorg. Chem.*, 2016, **55**, 10043–10056.

10 F. S. Guo, B. M. Day, Y. C. Chen, M. L. Tong, A. Mansikkamaki and R. A. Layfield, *Angew. Chem., Int. Ed.*, 2017, **56**, 11445–11449.

11 Y.-S. Ding, N. F. Chilton, R. E. P. Winpenny and Y.-Z. Zheng, *Angew. Chem., Int. Ed.*, 2016, **55**, 16071–16074.

12 F.-S. Guo, B. M. Day, Y.-C. Chen, M.-L. Tong, A. Mansikkamäki and R. A. Layfield, *Science*, 2018, **362**, 1400–1403.

13 O. Kahn, *Molecular Magnetism*, VCH Publications, New York, 1993.

14 (a) S. Hazra, S. Bhattacharya, M. K. Singh, L. Carrella, E. Rentschler, T. Weyhermueller, G. Rajaraman and S. Mohanta, *Inorg. Chem.*, 2013, **52**, 12881–12892; (b) S. Sasmal, S. Roy, L. Carrella, A. Jana, E. Rentschler and S. Mohanta, *Eur. J. Inorg. Chem.*, 2015, **2015**, 680–689; (c) S. Sasmal, S. Hazra, P. Kundu, S. Dutta, G. Rajaraman, E. C. Sañudo and S. Mohanta, *Inorg. Chem.*, 2011, **50**, 7257–7267; (d) S. Mohanta, K. K. Nanda, L. K. Thompson, U. Flörke and K. Nag, *Inorg. Chem.*, 1998, **37**, 1465–1472.

15 E. Ruiz, J. Cano, S. Alvarez and P. Alemany, *J. Am. Chem. Soc.*, 1998, **120**, 11122–11129.

16 J.-P. Costes, F. Dahan and A. Dupuis, *Inorg. Chem.*, 2000, **39**, 165–168.

17 (a) L. E. Roy and T. Hughbanks, *J. Am. Chem. Soc.*, 2006, **128**, 568–575; (b) G. Rajaraman, F. Totti, A. Bencini, A. Caneschi, R. Sessoli and D. Gatteschi, *Dalton Trans.*, 2009, 3153–3161; (c) S. K. Singh, N. K. Tibrewal and G. Rajaraman, *Dalton Trans.*, 2011, **40**, 10897–10906; (d) T. Rajeshkumar and G. Rajaraman, *Chem. Commun.*, 2012, **48**, 7856–7858; (e) M. K. Singh, T. Rajeshkumar, R. Kumar, S. K. Singh and G. Rajaraman, *Inorg. Chem.*, 2018, **57**, 1846–1858.

18 K. Zhang, D. Liu, V. Vieru, L. Hou, B. Cui, F.-S. Guo, L. F. Chibotaru and Y.-Y. Wang, *Dalton Trans.*, 2017, **46**, 638–642.

19 (a) O. Sun, P. Chen, H.-F. Li, T. Gao, W.-B. Sun, G.-M. Li and P.-F. Yan, *CrystEngComm*, 2016, **18**, 4627–4635; (b) J.-Y. Ge, H.-Y. Wang, J. Li, J.-Z. Xie, Y. Song and J.-L. Zuo, *Dalton Trans.*, 2017, **46**, 3353–3362.

20 (a) K. Katoh, R. Asano, A. Miura, Y. Horii, T. Morita, B. K. Breedlove and M. Yamashita, *Dalton Trans.*, 2014, **43**, 7716–7725; (b) T. Morita, M. Damjanovic, K. Katoh, Y. Kitagawa, N. Yasuda, Y. Lan, W. Wernsdorfer, B. K. Breedlove, M. Enders and M. Yamashita, *J. Am. Chem. Soc.*, 2018, **140**, 2995–3007; (c) J.-Y. Ge, H.-Y. Wang, J. Su, J. Li, B.-L. Wang, Y.-Q. Zhang and J.-L. Zuo, *Inorg. Chem.*, 2018, **57**, 1408–1416.

21 (a) K. L. M. Harriman, J. J. Le Roy, L. Ungur, R. J. Holmberg, I. Korobkov and M. Murugesu, *Chem. Sci.*, 2017, **8**, 231–240; (b) A.-J. Hutchings, F. Habib, R. J. Holmberg, I. Korobkov and M. Murugesu, *Inorg. Chem.*, 2014, **53**, 2102–2112; (c) L. Zhang, Y.-Q. Zhang, P. Zhang, L. Zhao, M. Guo and J. Tang, *Inorg. Chem.*, 2017, **56**, 7882–7889; (d) F.-S. Guo and R. A. Layfield, *Chem. Commun.*, 2017, **53**, 3130–3133; (e) Y. Qin, H. Zhang, H. Sun, Y. Pan, Y. Ge, Y. Li and Y.-Q. Zhang, *Chem.–Asian J.*, 2017, **12**, 2834–2844; (f) M. A. Dunstan, E. Rousset, M.-E. Boulon, R. W. Gable, L. Sorace and C. Boskovic, *Dalton Trans.*, 2017, **46**, 13756–

13767; (g) F. Gao, F.-L. Yang, G.-Z. Zhu and Y. Zhao, *Dalton Trans.*, 2015, **44**, 20230–20241.

22 (a) N. Ishikawa, M. Sugita, N. Tanaka, T. Ishikawa, S. Koshihara and Y. Kaizu, *Inorg. Chem.*, 2004, **43**, 5498–5500; (b) S. Takamatsu, T. Ishikawa, S. Koshihara and N. Ishikawa, *Inorg. Chem.*, 2007, **46**, 7250–7252; (c) N. Ishikawa, Y. Mizuno, S. Takamatsu, T. Ishikawa and S. Koshihara, *Inorg. Chem.*, 2008, **47**, 10217–10219; (d) N. Ishikawa, M. Sugita and W. Wernsdorfer, *Angew. Chem., Int. Ed.*, 2005, **44**, 2931–2935; (e) K. Wang, D. D. Qi, H. L. Wang, W. Cao, W. J. Li, T. Liu, C. Y. Duan and J. Z. Jiang, *Chem.–Eur. J.*, 2013, **19**, 11162–11166; (f) W. Cao, C. Gao, Y. Q. Zhang, D. D. Qi, T. Liu, K. Wang, C. Y. Duan, S. Gao and J. Z. Jiang, *Chem. Sci.*, 2015, **6**, 5947–5954; (g) K. Katoh, B. K. Breedlove and M. Yamashita, *Chem. Sci.*, 2016, **7**, 4329–4340; (h) A. Amokrane, S. Klyatskaya, M. Boero, M. Ruben and J. P. Bucher, *ACS Nano*, 2017, **11**, 10750–10760; (i) Y. X. Chen, F. Ma, X. X. Chen, B. W. Dong, K. Wang, S. D. Jiang, C. M. Wang, X. Chen, D. D. Qi, H. L. Sun, B. W. Wang, S. Gao and J. Z. Jiang, *Inorg. Chem.*, 2017, **56**, 13889–13896; (j) Y. X. Chen, F. Ma, X. X. Chen, B. W. Dong, K. Wang, S. D. Jiang, C. M. Wang, X. Chen, D. D. Qi, H. L. Sun, B. W. Wang, S. Gao and J. Z. Jiang, *Inorg. Chem. Front.*, 2017, **4**, 1465–1471.

23 (a) P. H. Lin, T. J. Burchell, R. Clerac and M. Murugesu, *Angew. Chem., Int. Ed.*, 2008, **47**, 8848–8851; (b) S. Q. Wu, Q. W. Xie, G. Y. An, X. Chen, C. M. Liu, A. L. Cui and H. Z. Kou, *Dalton Trans.*, 2013, **42**, 4369–4372; (c) S. Das, S. Hossain, A. Dey, S. Biswas, J. P. Sutterand and V. Chandrasekhar, *Inorg. Chem.*, 2014, **53**, 5020–5028; (d) P. H. Guo, Y. Meng, Y. C. Chen, Q. W. Li, B. Y. Wang, J. D. Leng, D. H. Bao, J. H. Jia and M. L. Tong, *J. Mater. Chem. C*, 2014, **2**, 8858–8864; (e) F. Gao, L. Cui, W. Liu, L. Hu, Y. W. Zhong, Y. Z. Li and J. L. Zuo, *Inorg. Chem.*, 2013, **52**, 11164–11172; (f) H. Oshio, N. Hoshino, T. Ito and M. Nakano, *J. Am. Chem. Soc.*, 2004, **126**, 8805–8812; (g) Y. N. Guo, G. F. Xu, W. Wernsdorfer, L. Ungur, Y. Guo, J. K. Tang, H. J. Zhang, L. F. Chibotaru and A. K. Powell, *J. Am. Chem. Soc.*, 2011, **133**, 11948–11951; (h) X. L. Li, J. F. Wu, L. Zhao, W. Shi, P. Cheng and J. K. Tang, *Chem. Commun.*, 2017, **53**, 3026–3029; (i) H. M. Dong, Y. Li, Z. Y. Liu, E. C. Yang and X. J. Zhao, *Dalton Trans.*, 2016, **45**, 11876–11882.

24 (a) G. J. Chen, Y. N. Guo, J. L. Tian, J. K. Tang, W. Gu, X. Liu, S. P. Yan, P. Cheng and D. Z. Liao, *Chem.–Eur. J.*, 2012, **18**, 2484–2487; (b) D. P. Li, X. P. Zhang, T. W. Wang, B. B. Ma, C. H. Li, Y. Z. Li and X. Z. You, *Chem. Commun.*, 2011, **47**, 6867–6869; (c) F. Pointillart, K. Bernot, G. Poneti and R. Sessoli, *Inorg. Chem.*, 2012, **51**, 12218–12229; (d) F. Pointillart, S. Klementieva, V. Kuropatov, Y. L. Gal, S. Golhen, O. Cador, V. Cherkasov and L. Ouahab, *Chem. Commun.*, 2012, **48**, 714–716; (e) P. Totaro, K. C. M. Westrup, Ma. E. Boulon, G. G. Nunes, D. F. Back, A. Barison, S. Ciattini, M. Mannini, L. Sorace, J. F. Soares, A. Corniad and R. Sessoli, *Dalton Trans.*, 2013, **42**, 4416–4426; (f) Y. P. Dong, P. F. Yan, X. Y. Zou and G. M. Li, *Inorg. Chem. Front.*, 2015, **2**, 827–836; (g) P. P. Cen,

S. Zhang, X. Y. Liu, W. M. Song, Y. Q. Zhang, G. Xie and S. P. Chen, *Inorg. Chem.*, 2017, **56**, 3644–3656; (*h*) X. H. Yi, G. Calvez, C. Daiguebonne, O. Guillou and K. Bernot, *Inorg. Chem.*, 2015, **54**, 5213–5219; (*i*) J. R. Jiménez, I. F. D. Ortega, E. Ruiz, D. Aravena, S. J. A. Pope, E. Colacio and J. M. Herrera, *Chem.–Eur. J.*, 2016, **22**, 14548–14559.

25 (*a*) Z. L. Wu, J. Dong, W. Y. Ni, B. W. Zhang, J. Z. Cui and B. Zhao, *Dalton Trans.*, 2014, **43**, 16838–16845; (*b*) L. Jia, Q. Chen, Y. S. Meng, H. L. Sun and S. Gao, *Chem. Commun.*, 2014, **50**, 6052–6055; (*c*) Y. L. Wang, C. B. Han, Y. Q. Zhang, Q. Y. Liu, C. M. Liu and S. G. Yin, *Inorg. Chem.*, 2016, **55**, 5578–5584; (*d*) A. R. Barón, I. Oyarzabal, F. M. A. Campos, J. M. Seco, A. R. Diéguez and I. Fernández, *Inorg. Chem.*, 2017, **56**, 8768–8775; (*e*) E. C. Mazarakioti, J. Regier, L. C. Silva, W. Wernsdorfer, M. Pilkington, J. K. Tang and T. C. Stamatatos, *Inorg. Chem.*, 2017, **56**, 3568–3578; (*f*) R. P. Li, Q. Y. Liu, Y. L. Wang, C. M. Liu and S. J. Liu, *Inorg. Chem. Front.*, 2017, **4**, 1149–1156; (*g*) G. J. Zhou, Y. S. Ding and Y. Z. Zheng, *Dalton Trans.*, 2017, **46**, 3100–3104; (*h*) X. J. Zhang, V. Vieru, X. W. Feng, J. L. Liu, Z. J. Zhang, B. Na, W. Shi, B. W. Wang, A. K. Powell, L. F. Chibotaru, S. Gao, P. Cheng and J. R. Long, *Angew. Chem., Int. Ed.*, 2015, **54**, 9861–9865.

26 G. M. Sheldrick, *SADABS*, Universität Göttingen, Germany, 2011.

27 (*a*) G. M. Sheldrick, *Acta Crystallogr., Sect. C: Struct. Chem.*, 2015, **71**, 3–8; (*b*) G. M. Sheldrick, *Acta Crystallogr., Sect. A: Found. Crystallogr.*, 2008, **64**, 112–122.

28 F. Aquilante, L. De Vico, N. Ferre, G. Ghigo, P. A. Malmqvist, P. Neogrady, T. B. Pedersen, M. Pitonak, M. Reiher, B. O. Roos, L. Serrano-Andres, M. Urban, V. Veryazov and R. Lindh, *J. Comput. Chem.*, 2010, **31**, 224–247.

29 F. Aquilante, J. Autschbach, R. K. Carlson, L. F. Chibotaru, M. G. Delcey, L. De Vico, I. Fdez Galvan, N. Ferre, L. M. Frutos, L. Gagliardi, M. Garavelli, A. Giussani, C. E. Hoyer, G. Li Manni, H. Lischka, D. Ma, P. A. Malmqvist, T. Muller, A. Nenov, M. Olivucci, T. B. Pedersen, D. Peng, F. Plasser, B. Pritchard, M. Reiher, I. Rivalta, I. Schapiro, J. Segarra-Marti, M. Stenrup, D. G. Truhlar, L. Ungur, A. Valentini, S. Vancoillie, V. Veryazov, V. P. Vysotskiy, O. Weingart, F. Zapata and R. Lindh, *J. Comput. Chem.*, 2016, **37**, 506–541.

30 B. O. Roos, R. Lindh, P. Malmqvist, V. Veryazov and P. Widmark, *J. Phys. Chem. A*, 2005, **109**, 6575–6579.

31 S. A. Sulway, R. A. Layfield, F. Tuna, W. Wernsdorfer and R. E. P. Winpenny, *Chem. Commun.*, 2012, **48**, 1508–1510.

32 (*a*) J. Tang, I. Hewitt, N. T. Madhu, G. Chastanet, W. Wernsdorfer, C. E. Anson, C. Benelli, R. Sessoli and A. K. Powell, *Angew. Chem., Int. Ed.*, 2006, **45**, 1729–1733; (*b*) X. Yi, K. Bernot, F. Pointillart, G. Poneti, G. Calvez, C. Daiguebonne, O. Guillou and R. Sessoli, *Chem.–Eur. J.*, 2012, **18**, 11379–11387; (*c*) F. Pointillart, B. Le Guennic, O. Maury, S. Golhen, O. Cador and L. Ouahab, *Inorg. Chem.*, 2013, **52**, 1398–1408.

33 J. r. m. Long, F. Habib, P.-H. Lin, I. Korobkov, G. Enright, L. Ungur, W. Wernsdorfer, L. F. Chibotaru and M. Murugesu, *J. Am. Chem. Soc.*, 2011, **133**, 5319–5328.

34 (*a*) Y. Ma, G.-F. Xu, X. Yang, L.-C. Li, J. Tang, S.-P. Yan, P. Cheng and D.-Z. Liao, *Chem. Commun.*, 2010, **46**, 8264–8266; (*b*) N. Ishikawa, T. Iino and Y. Kaizu, *J. Am. Chem. Soc.*, 2002, **124**, 11440–11447; (*c*) M. Jeletic, P.-H. Lin, J. J. Le Roy, I. Korobkov, S. I. Gorelsky and M. Murugesu, *J. Am. Chem. Soc.*, 2011, **133**, 19286–19289; (*d*) F. Habib, P.-H. Lin, J. Long, I. Korobkov, W. Wernsdorfer and M. Murugesu, *J. Am. Chem. Soc.*, 2011, **133**, 8830–8833.

35 (*a*) W. Wernsdorfer, S. Bhaduri, C. Boskovic, G. Christou and D. N. Hendrickson, *Phys. Rev. B: Condens. Matter Mater. Phys.*, 2002, **65**, 180403; (*b*) W. Wernsdorfer, N. E. Chakov and G. Christou, *Phys. Rev. Lett.*, 2005, **95**, 037203.

36 (*a*) K. S. Cole and R. H. J. Cole, *J. Chem. Phys.*, 1941, **9**, 341–351; (*b*) S. M. J. Aubin, Z. Sun, L. Pardi, J. Krzystek, K. Folting, L.-C. Brunel, A. L. Rheingold, G. Christou and D. N. Hendrickson, *Inorg. Chem.*, 1999, **38**, 5329–5340.

37 S. Titos-Padilla, J. Ruiz, J. M. Herrera, E. K. Brechin, W. Wersndorfer, F. Lloret and E. Colacio, *Inorg. Chem.*, 2013, **52**, 9620–9626.

38 J. L. Liu, K. Yuan, J. D. Leng, L. Ungur, W. Wernsdorfer, F. S. Guo, L. F. Chibotaru and M. L. Tong, *Inorg. Chem.*, 2012, **51**, 8538–8544.

39 E. Colacio, J. Ruiz, E. Ruiz, E. Cremades, J. Krzystek, S. Carretta, J. Cano, T. Guidi, W. Wernsdorfer and E. K. Brechin, *Angew. Chem., Int. Ed.*, 2013, **52**, 9130–9134.

40 (*a*) M. Nematirad, W. J. Gee, S. K. Langley, N. F. Chilton, B. Moubaraki, K. S. Murray and S. R. Batten, *Dalton Trans.*, 2012, **41**, 13711–13715; (*b*) L. Zhao, J. Wu, H. Ke and J. Tang, *CrystEngComm*, 2013, **15**, 5301–5306; (*c*) Z. Jiang, L. Sun, Q. Yang, S. Wei, H. Ke, S. Chen, Y. Zhang, Q. Wei and G. Xie, *CrystEngComm*, 2017, **19**, 5735–5741.

41 (*a*) W. B. Sun, B. Yan, L. H. Jia, B. W. Wang, Q. Zhang, X. Cheng, H. F. Li, P. Chen, Z. M. Wang and S. Gao, *Dalton Trans.*, 2016, **45**, 8790–8794; (*b*) Y. Ge, Y. Qin, Y. Cui, Y. Pan, Y. Huang, Y. Li, W. Liu and Y.-Q. Zhang, *Chem.–Asian J.*, 2018, **13**, 3753–3761; (*c*) W. Huang, F. X. Shen, S. Q. Wu, L. Liu, D. Y. Wu, Z. Zheng, J. Xu, M. Zhang, X. C. Huang, J. Jiang, F. F. Pan, Y. Li, K. Zhu and O. Sato, *Inorg. Chem.*, 2016, **55**, 5476–5484; (*d*) J. Y. Ge, L. Cui, J. Li, F. Yu, Y. Song, Y. Q. Zhang, J. L. Zuo and M. Kurmoo, *Inorg. Chem.*, 2017, **56**, 336–343; (*e*) F. Ma, Q. Chen, J. Xiong, H. L. Sun, Y. Q. Zhang and S. Gao, *Inorg. Chem.*, 2017, **56**, 13430–13436.

42 (*a*) L. F. Chibotaru, L. Ungur and A. Soncini, *Angew. Chem., Int. Ed.*, 2008, **47**, 4126–4129; (*b*) L. Ungur, W. Van den Heuvel and L. F. Chibotaru, *New J. Chem.*, 2009, **33**, 1224–1230; (*c*) L. F. Chibotaru, L. Ungur, C. Aronica, H. Elmoll, G. Pileta and D. Luneau, *J. Am. Chem. Soc.*, 2008, **130**, 12445–12455.

43 M. E. Lines, *J. Chem. Phys.*, 1971, **55**, 2977–2984.

44 K. C. Mondal, A. Sundt, Y. H. Lan, G. E. Kostakis, O. Waldmann, L. Ungur, L. F. Chibotaru, C. E. Anson and A. K. Powell, *Angew. Chem., Int. Ed.*, 2012, **51**, 7550–7554.